

pubs.acs.org/JACS Communication

Ultraviolet Photodissociation Mass Spectrometry Captures the Acyl Chain Length-Dependent Conformation Dynamics of Acyl Carrier Protein

Yuanzhi Xie, [#] Zheyi Liu, [#] Huiwen Qin, Heng Zhao, Weiqing Zhang, Chunlei Xiao, Xian Wang, ^{*} Xueming Yang, and Fangjun Wang*



Cite This: J. Am. Chem. Soc. 2025, 147, 16760–16765



ACCESS I

III Metrics & More

Article Recommendations

s Supporting Information

ABSTRACT: Capturing the acyl chain dependent conformation dynamics of acyl carrier protein (ACP) is critical for understanding the molecular mechanism of acyl chain stabilization and elongation, providing structural insights for ACP evolution. Herein, we utilize native mass spectrometry (nMS) and 193 nm ultraviolet photodissociation (UVPD) to systematically interrogate the structural details in activation and interactions of ACP with C4–C18 acyl chains. The unstable acyl-ACP intermediates can be isolated and subjected to high-sensitivity UVPD analysis individually without matrix interference. We find that the acyl chains mainly insert into ACP subpocket I until the chain length surpasses the cavity's maximum capacity by 10 carbons. Then, the hydrophobic part of long acyl chains (>C10) bends into subpocket II. Notably, Phe50 and Ile62 play a critical role in regulating the size of the hydrophobic pocket, while Loop I and Thr64-Gln66 are essential for stabilizing long-chain acyl-ACPs. Our findings pave the way for ACP rational evolution to promote the biosynthesis of target fatty acids.

s global energy demand continues to grow, sustainable Aenergy alternatives to fossil fuels have become urgent needs. A promising strategy is the direct production of oleochemicals by microbial synthesis. The industrial microorganism Escherichia coli (E. coli) is well-suited for this purpose, as it can generate free fatty acids (FFAs) from various carbon substrates. Medium-chain fatty acids (MCFAs, C8-C12) are promising precursors for gasoline and aviation fuel due to their unique physicochemical properties.^{2,3} However, most microorganisms naturally produce FFAs predominantly as long-chain fatty acids (LCFAs, C14-C18).4 To enhance MCFA production, engineered strains are often supplemented with heterologous plant thioesterases (TEs), which hydrolyze acyl intermediates to release MCFAs. However, it is still challenging to efficiently modulate the hydrolysis of fatty acyl intermediates to promote the MCFA production.

Acyl carrier proteins (ACPs) are primary carriers of nascent FA chains.⁶ Recent studies suggest that they are not only transporters but also critical determinants of acyl chain length in FA synthesis.⁷ To perform their roles in FA synthesis, the hydroxyl group on conserved residue Ser36 of inactive apo-ACP is covalently modified with 4'-phosphopantetheine (4'-PP) by ACP synthase, forms a phosphodiester bond, and converts apo-ACP into its active holo-form.⁸ The 4'-PP free thiol group of holo-ACP then serves as the attachment point for covalent binding to the acyl chains to form acyl-ACP intermediates (Figure S1). The acyl chains are produced by an iterative series of reactions, and the chain length is elongated by two carbon atoms per cycle until hydrolysis by TEs to generate FFAs (Figure S2).⁹ The functional structure, especially the ACP hydrophobic pocket and the flexibility of

the 4'-PP group are crucial to the acyl chain stabilization and elongation. Although many efforts have been made to improve the selectivity of TEs for MCFA production, how to evolve the ACP conformations to promote MCFA generation is still unknown due to the unclear acyl chain length-dependent conformation dynamics of acyl-ACPs.

Recently, the crystal structures of butyryl (C4), hexanoyl (C6), heptanoyl (C7), and decanoyl (C10)-ACPs have been elucidated, suggesting the saturated acyl chains are sequestered in the ACP hydrophobic cavity and interact with the side chains of hydrophobic residues, thereby preventing the thioester part from being hydrolyzed. 11,12 Furthermore, ACPs exhibit conformational adaptability to accommodate varying acyl chain lengths, with the hydrophobic cavity optimally fitting chains up to eight carbon atoms. 13 However, the acyl-ACPs with longer chains (>C10) are unstable and hard to crystallize for structure characterization. On the other hand, Sztain et al. demonstrated the importance of ACP conformational changes in the high-specific recognition with partner enzymes by nuclear magnetic resonance (NMR) and molecular dynamics (MD) simulation.¹⁴ However, abundant acyl attachment enzyme (AasS) and FFAs were added into the acyl-ACP samples to prevent the inevitable hydrolysis of fragile thioester during the long-time NMR data collection,

Received: February 25, 2025
Revised: May 7, 2025
Accepted: May 7, 2025
Published: May 12, 2025





introducing high matrix interference. Therefore, a highly selective, sensitive, and rapid tool is needed to probe the conformational differences of acyl-ACPs with different acyl chain lengths.

Native mass spectrometry (nMS) introduces proteins or protein complexes into the gas phase via nondenaturing electrospray ionization (nESI), preserving their native-like compact structures and interactions. 15,16 nMS enables highthroughput profiling of stoichiometry, assembly, and dissociation constants of protein-protein and protein-ligand complexes. 17,18 When coupled with 193 nm ultraviolet photodissociation (UVPD) to generate rich types of structure-informative fragments, the nMS-UVPD strategy can effectively examine the subtle alterations in protein structures. 19-22 Recent studies indicate the 193 nm photodissociation is more efficient than conventional collision induced dissociations (HCD/CID) in the fragmentation of native-like protein ions.²³ The dynamic structural insights into protein conformation alterations and protein-ligand interactions can be successfully probed by nMS coupled with 193 nm UVPD analysis. 24,25 Compared with previous bottom-up structural MS strategies with chemical labeling that can only provide the structural information on labeled residues, the native top-down MS (nTDMS) analysis with 193 nm UVPD can probe the local structural alterations of all types of residues.26

In this study, we utilized nMS and 193 nm UVPD to interrogate the structural features of C4—C18 acyl-ACPs individually. Our structural MS strategy can selectively isolate the unstable acyl-ACPs for UVPD analysis to get structural details, without the influences of extra AasS and FFAs (Figure 1).

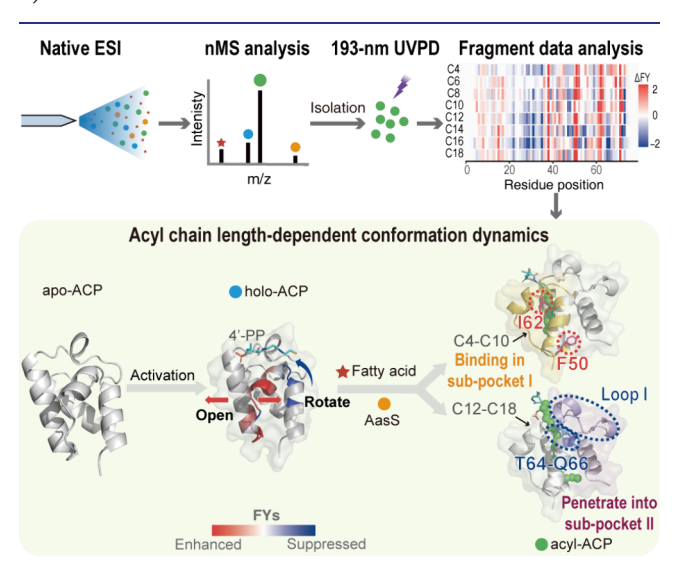


Figure 1. nMS and UVPD exploration of the conformation dynamics of C4–C18 acyl-ACP intermediates with high selectivity and sensitivity.

At first, apo (inactive form), holo (active form), and acyl (acyl-substrate modified forms) ACPs were clearly detected in the nMS spectra of different ACP samples (Figure 2a). Similar narrow charge state distributions (CSDs) were observed for all ACP species with the dominant charge state of 5+ (Figure 2a), suggesting the compact structures of these ACP forms are retained in "native-like" states.²⁷ Due to their significant

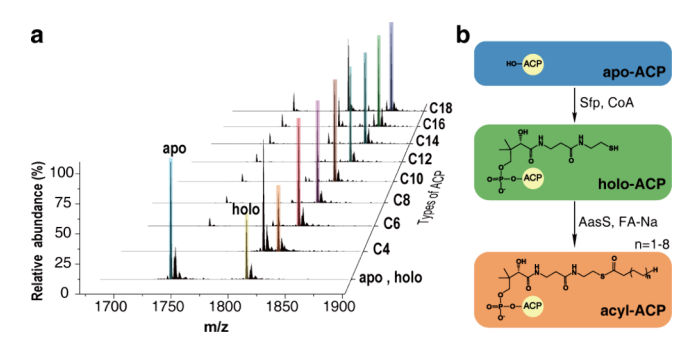


Figure 2. (a) Mass spectra of apo-, holo-, and C4—C18 acyl-ACP ions in nMS analysis. (b) The post-translational manipulations and modifications of ACPs.

molecular weight differences, ACP ions (9 kDa) can be efficiently isolated from coexisting FFAs (<300 Da) and AasS (60 kDa). Thus, unstable acyl-ACP intermediates can be selectively trapped in the MS dissociation chamber for UVPD-based structural analysis, minimizing the interference from other species. For each of the ACP forms, the most abundant charge state (5+) was subjected to 193 nm UVPD, generating diverse structure-informative fragments. Notably, over 375 fragment ions could be confidently matched, achieving sequence coverage exceeding 93% for all examined ACP forms (Figures S3–S5).

The inactive apo-ACP requires modification with the 4'-PP group at Ser36 to become active holo-ACP (Figure 2b). We then applied 193 nm UVPD to explore the structural impact of this modification based on the differences in residue fragment yields (FYs) between apo- and holo-ACPs. Generally, residue FYs are linked to local flexibility or rigidity, primarily resulting from alterations of intra- or intermolecular interactions. Residues with higher flexibility or fewer local interactions typically exhibit higher FYs; conversely, FY decrease generally occurs when local interactions and stability are enhanced.^{28,29} As reported in previous NMR studies, the structures of apoand holo-ACPs were basically similar and the chemical shifts between them were not significantly different, 30,31 suggesting that the modification of the 4'-PP group has little influence on the ACP structure. However, our UVPD analysis results indicated a conformational transition from a closed to a more open structure following 4'-PP modification, as indicated by the generally increased residue FYs of holo-ACP compared to the apo form (Figure 3a). This can be attributed to the overall expansion of ACP hydrophobic cavity, which is essential for the acyl chain adaptation in stabilizing the acyl-ACP intermediates. 12 Particularly, the substantial and collective residue FY increase in Loop II and nearby regions is consistent with the expansion of cleft within Helix II-III (Figure 3b), resulting in Helix III far away from Helix II.³² These conformational changes provide additional space for acyl chains to enter the ACP hydrophobic pocket. 32,3

Notably, the residues in Loop III (Ile62-Gln66) show significantly decreased FYs compared to the increased FYs near the C-terminal region of Helix IV. This may arise from hydrogen bonds formed between the polar groups of 4'-PP and the hydroxyl side chains of Thr63 and Thr64, 12 as the C-terminal region of Helix IV is displaced away from Helix II, thereby weakening its interactions with neighboring residues. These conformational adjustments suggest a rotational movement in Loop III (Figure 3b). This structural reorganization not only strengthens hydrophobic interactions between the

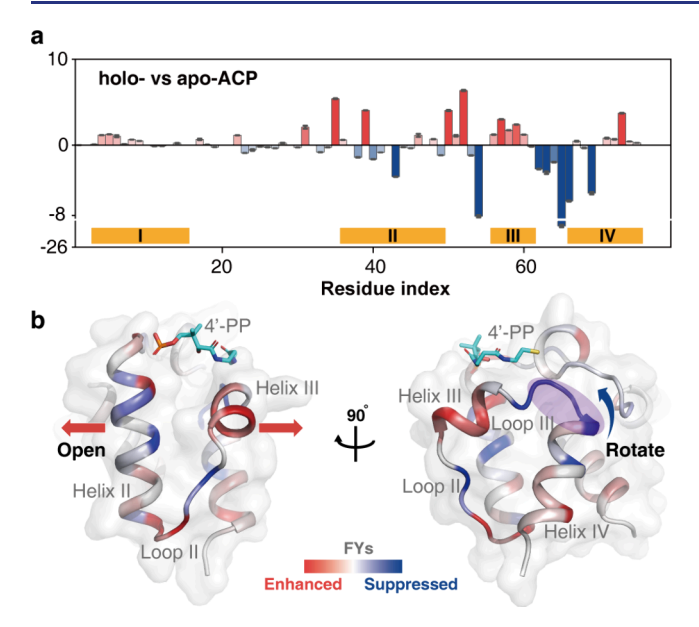


Figure 3. UVPD analysis of the impact of 4'-PP on ACP structure. (a) The relative changes in residue FY between apo- and holo-ACPs. The α -helical regions of ACP are marked in orange. (b) The locations of residues and regions with significant FY changes in ACP crystal structure, modified from PDB ID: 2FAD.

hydrophobic portions of the threonine side chains and surrounding hydrophobic residues such as Ile62, Val65, and Ile69 but also enlarges the capacity of the ACP hydrophobic cavity. Similar conformational changes were also reported by Arya et al.³²

In the FFA biosynthesis process, holo-ACP transports FFAs with varying chain lengths via its 4'-PP group through the formation of fragile thioester bonds (Figure S1). Understanding the structural features of acyl-ACP intermediates in relation to acyl chain length is crucial for comprehending how holo-ACP stabilizes and regulates the acyl chain enlongation.

Therefore, holo- and acyl-ACPs with different acyl chain lengths were characterized by 193 nm UVPD, and the residue FYs were systematically compared across different forms. Generally, we observed varying degrees of alterations in residue FYs across different regions of acyl-ACPs (Figure S6), suggesting that both unfolding and refolding occurred in this process. These structural modulations enable ACPs to dynamically accommodate the elongation of acyl chains while effectively shielding the hydrophobic moieties from solvent exposure, thereby facilitating their efficient transport to enzymes of FFA synthesis. 34,35 These observations align with the results of 500 ns MD simulation conducted by Sztain et al. 14 The FYs of Phe50-Thr52 at the base of the hydrophobic pocket exhibited a significant increase, indicating increased conformational flexibility in this region (Figure 4a). This structural loosening can be attributed to the expanded hydrophobic core of acyl-ACPs compared to their holoforms, which creates steric accommodation for acyl chain elongation.^{36,37} Interestingly, Phe50 shows a consistent FY increase across all acyl-ACPs. This observation agrees with previous mechanistic studies of medium/short-chain acyl-ACPs, which propose that Phe50 undergoes lateral displacement to permit acyl chain ingress (Figure 4b).³⁸ Our findings extend the mechanistic framework to long-chain acyl-ACP systems while providing direct experimental validation of Phe50's pivotal role as a conformational gatekeeper during acyl chain accommodation.

The negatively charged residues on Helix II (known as recognition Helix) play important roles in the interactions between acyl-ACPs with partner enzymes.³⁹ The three consecutive Glu residues (Glu47-Glu49) at the C-terminus of Helix II showed significant FY decreases in acyl-ACPs, consistent with the fluctuations observed in MD simulations (Figure 4b). 40 This may be due to conformational changes induced by the alterations of Phe50 position, which implies a more compact local structure with higher negative charge density. Meanwhile, differences in the physicochemical proper-

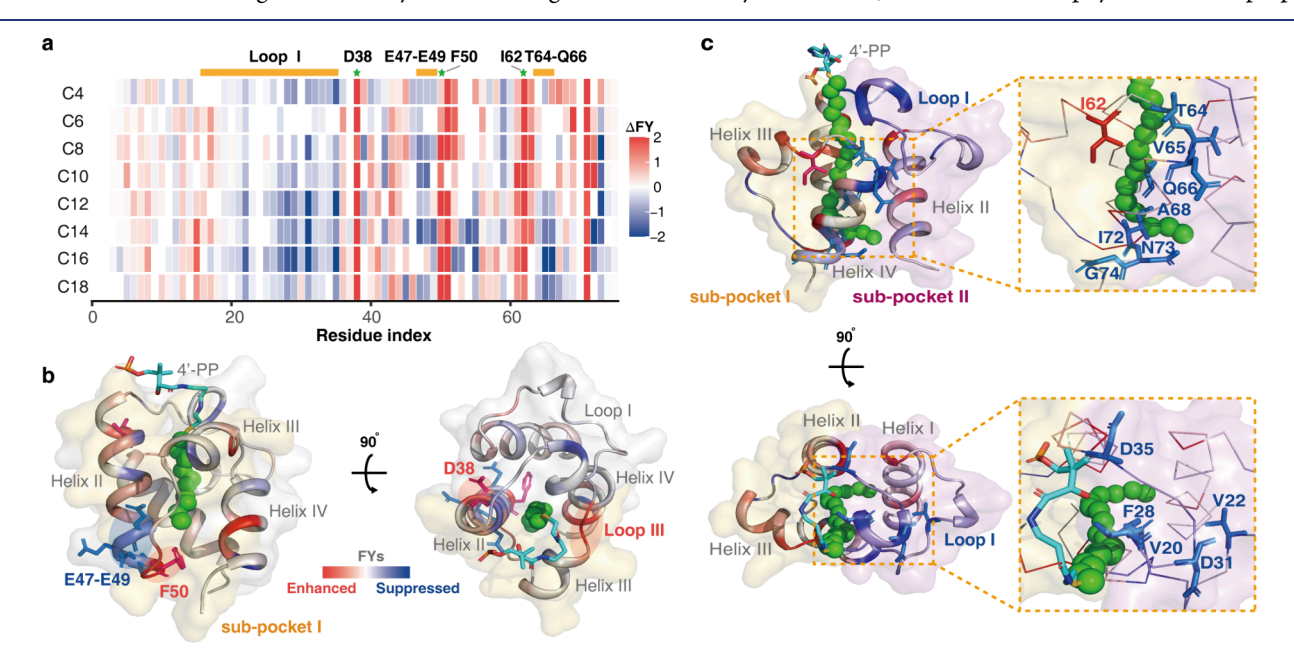


Figure 4. (a) Heat map showing relative changes in residue FY between holo- and acyl-ACPs. (b) The regions with significant FY alterations in all acyl-ACPs. (c) The hotspots in stabilizing long-chain (C12-C18) acyl-ACPs, with subpocket I labeled in yellow orange and subpocket II labeled in violet. The residues with increased and decreased FYs are labeled as red and blue in the ACP structure (PDB ID: 2FAE), respectively.

ties of this region among different chain lengths are reflected in the strength of specific binding to different partner enzymes. Conversely, Asp38 exhibited a notable FY increase across all acyl-ACPs (Figure 4a). This is likely due to the acyl chain enhancing the flexibility of the N-terminal region of Helix II, facilitating more effective interactions with surrounding hydrophobic residues (Figure 4b). The increased flexibility enables greater exposure of Asp38 on the protein surface, thereby facilitating recognition by β -ketoacyl ACP synthase I (FabB), which is the partner enzyme involved in the initial step of fatty acid chain elongation (Figure S2).⁴¹ These findings strongly support the "Specificity Control" theory proposed by Buyachuihan et al., which posits that acyl substrates regulate the localization and function of ACPs through their interactions with ACPs. 42

The FYs of Lys61-Thr63 on Loop III displayed biphasic modulation: a marked decrease in residue FYs following ACP activation, followed by a significant increase upon acyl chain loading (Figure 4a). This dynamic response correlates with the structural role of Loop III in gating the hydrophobic pocket entrance. Notably, Ile62 within this motif exhibits consistent FY increase across all acyl-ACPs, supporting its function as a structural rheostat that modulates entrance aperture dimensions while stabilizing the accommodated acyl chain (Figure 4c). These findings are corroborated by crystallographic evidence demonstrating Ile62's positional adaptability during substrate binding, collectively validating its critical role in maintaining the pocket's structural plasticity. 11 A previous MD simulation study on ACP conformations suggested that the ACP binding cavity can be divided into two distinct subpockets sharing a common entrance including subpocket I (Ser36-Gln76) and subpocket II (Ile3-Glu49, Gln66-Gln76).40 Thus, our findings demonstrate the acyl chain binding predominantly occurs in subpocket I (Figure 4c), consistent with the observations of crystal and NMR structures. 11,43

Through comparative analysis of acyl-ACPs with different chain lengths, we identified a chain length-dependent inflection point at C10: acyl-ACPs, exceeding this length, exhibited a pronounced decrease of FYs in Loop I and Thr64-Gln66 regions (Figure 4a). This FY decrease pattern correlates with the known maximal packing capacity (C10) of the ACP hydrophobic pocket, indicating a chain length-dependent conformational reorganization in long-chain acyl-ACP (>C10). 12 We propose that supernumerary carbons (>C10) displace the thioester moiety beyond the pocket's protective boundary, thereby enhancing its solvent accessibility and hydrolytic susceptibility (Figure 4c). This is evidenced by decreased FYs at the Thr64-Gln66 region. To circumvent steric constraints, the long acyl chains adopt bent or folded conformations within the expanded cavity. Such structural adaptations drive two synergistic effects: (i) widening the entrance via Loop III remodeling and (ii) enhancing van der Waals contacts between kinked acyl chains and hydrophobic residues, collectively explaining the FY decreases at the Loop III/Helix IV interface. Furthermore, the decreased FYs in Loop I suggest that compensatory conformational shifts may facilitate partial accommodation of overlong chains within auxiliary subpocket II. These insights suggest that targeted mutagenesis of dynamic residues at Loop I and C-terminal region of Loop III could destabilize long-chain acyl-ACPs by disrupting adaptive stabilization effects, which might promote the biosynthesis of MCFAs.

Overall, in this study, we utilized nMS to isolate the acyl-ACP intermediates individually for subsequent 193 nm UVPD structural analysis. By eliminating interference from coexisting AasS and FFAs, we can observe subtle conformational changes during ACP activation and its interactions with C4-C18 acyl chains, which are difficult to capture by the existing tools. Our findings highlight Ile62, located at the pocket entrance, and Phe50, located at the bottom, as potential hotspots for regulating the entry of acyl-ACP intermediates. Meanwhile, Loop I and Thr64-Gln66 play critical roles in stabilizing longchain (C12-C18) acyl-ACPs. Our results not only demonstrate the unique advantage of nMS and 193 nm UVPD in interrogating conformation dynamics of unstable acyl-ACP intermediates but also provide essential structural insights for the rational evolution of ACPs to promote the biosynthesis of target FFAs.

ASSOCIATED CONTENT

Supporting Information

The Supporting Information is available free of charge at https://pubs.acs.org/doi/10.1021/jacs.5c03426.

Structure of 4'-pp, schematic of fatty acid biosynthesis, fragmentation yields of ACPs, UVPD spectra of ACPs, sequence cleavage coverages, the residue FY changes between holo- and acyl-ACPs, materials and methods, flowchart for the acquisition, and processing of UVPD data sets (PDF)

AUTHOR INFORMATION

Corresponding Authors

Fangjun Wang – State Key Laboratory of Chemical Reaction Dynamics, Dalian Institute of Chemical Physics, Chinese Academy of Sciences, Dalian 116023, China; University of Chinese Academy of Sciences, Beijing 100049, China; orcid.org/0000-0002-8118-7019; Email: wangfj@ dicp.ac.cn

Xian Wang - School of Chemistry and Materials Science, South-Central Minzu University, Wuhan 430074, China; Email: xwang27@mail.scuec.edu.cn

Authors

Yuanzhi Xie - School of Chemistry and Materials Science, South-Central Minzu University, Wuhan 430074, China; State Key Laboratory of Chemical Reaction Dynamics, Dalian Institute of Chemical Physics, Chinese Academy of Sciences, Dalian 116023, China

Zheyi Liu - State Key Laboratory of Chemical Reaction Dynamics, Dalian Institute of Chemical Physics, Chinese Academy of Sciences, Dalian 116023, China; University of Chinese Academy of Sciences, Beijing 100049, China

Huiwen Qin - State Key Laboratory of Chemical Reaction Dynamics, Dalian Institute of Chemical Physics, Chinese Academy of Sciences, Dalian 116023, China; University of Chinese Academy of Sciences, Beijing 100049, China

Heng Zhao - State Key Laboratory of Chemical Reaction Dynamics, Dalian Institute of Chemical Physics, Chinese Academy of Sciences, Dalian 116023, China

Weiqing Zhang — State Key Laboratory of Chemical Reaction Dynamics, Dalian Institute of Chemical Physics, Chinese Academy of Sciences, Dalian 116023, China; University of Chinese Academy of Sciences, Beijing 100049, China; orcid.org/0000-0001-6518-4152

Chunlei Xiao — State Key Laboratory of Chemical Reaction Dynamics, Dalian Institute of Chemical Physics, Chinese Academy of Sciences, Dalian 116023, China; University of Chinese Academy of Sciences, Beijing 100049, China; orcid.org/0000-0002-1549-5945

Xueming Yang — State Key Laboratory of Chemical Reaction Dynamics, Dalian Institute of Chemical Physics, Chinese Academy of Sciences, Dalian 116023, China; University of Chinese Academy of Sciences, Beijing 100049, China; orcid.org/0000-0001-6684-9187

Complete contact information is available at: https://pubs.acs.org/10.1021/jacs.5c03426

Author Contributions

"Y.X. and Z.L. contributed equally.

Notes

The authors declare no competing financial interest.

ACKNOWLEDGMENTS

We acknowledge the financial support by the National Key R&D Program of China (2022YFA1304601, 2022YFC3400502), the National Natural Science Foundation of China (32088101, 92253304, 22288201, 22276221), and the Strategic Priority Research Program of the Chinese Academy of Sciences (XDB0970100) and the grants from DICP (DICP I202242, DICP I202228). We thank the staff members of the Biological Mass Spectrometry System (https://cstr.cn/31127.02.DCLS.ESBMS) at the Dalian Coherent Light Source (https://cstr.cn/31127.02.DCLS) for providing technical support and assistance in data collection and analysis.

■ REFERENCES

- (1) Zhao, C. H.; Zhang, Y. P.; Li, Y. Production of fuels and chemicals from renewable resources using engineered. *Biotechnol. Adv.* **2019**, *37* (7), 107402.
- (2) He, M. L.; Wang, M.; Tang, G. L.; Fang, Y. M.; Tan, T. W. From medium chain fatty alcohol to jet fuel: Rational integration of selective dehydration and hydro-processing. *APPL CATAL A-GEN* **2018**, *550*, 160–167.
- (3) Jiménez-Díaz, L.; Caballero, A.; Pérez-Hernández, N.; Segura, A. Microbial alkane production for jet fuel industry: motivation, state of the art and perspectives. *Microb. Biotechnol.* **2017**, *10* (1), 103–124.
- (4) Choi, Y. J.; Lee, S. Y. Microbial production of short-chain alkanes. *Nature* **2013**, *502* (7472), *571*–*574*.
- (5) Grisewood, M. J.; Hernández-Lozada, N. J.; Thoden, J. B.; Gifford, N. P.; Mendez-Perez, D.; Schoenberger, H. A.; Allan, M. F.; Floy, M. E.; Lai, R. Y.; Holden, H. M.; Pfleger, B. F.; Maranas, C. D. Computational Redesign of Acyl-ACP Thioesterase with Improved Selectivity toward Medium-Chain-Length Fatty Acids. *ACS Catal.* 2017, 7 (6), 3837–3849.
- (6) Crosby, J.; Crump, M. P. The structural role of the carrier protein active controller or passive carrier. *Nat. Prod. Rep.* **2012**, 29 (10), 1111–1137.
- (7) Heil, C. S.; Wehrheim, S. S.; Paithankar, K. S.; Grininger, M. Fatty Acid Biosynthesis: Chain-Length Regulation and Control. *ChemBioChem.* **2019**, 20 (18), 2298–2321.
- (8) Flugel, R. S.; Hwangbo, Y.; Lambalot, R. H.; Cronan, J. E.; Walsh, C. T. Holo-(acyl carrier protein) synthase and phosphopantetheinyl transfer in. *J. Biol. Chem.* **2000**, *275* (2), 959–968.
- (9) Ruppe, A.; Fox, J. M. Analysis of Interdependent Kinetic Controls of Fatty Acid Synthases. *ACS Catal.* **2018**, 8 (12), 11722–11734.

- (10) Byers, D. M.; Gong, H. S. Acyl carrier protein: structure-function relationships in a conserved multifunctional protein family. *Biochem. Cell Biol.* **2007**, 85 (6), 649–662.
- (11) Roujeinikova, A.; Baldock, C.; Simon, W. J.; Gilroy, J.; Baker, P. J.; Stuitje, A. R.; Rice, D. W.; Slabas, A. R.; Rafferty, J. B. X-ray crystallographic studies on butyryl-ACP reveal flexibility of the structure around a putative acyl chain binding site. *Structure* **2002**, *10* (6), 825–835.
- (12) Roujeinikova, A.; Simon, W. J.; Gilroy, J.; Rice, D. W.; Rafferty, J. B.; Slabas, A. R. Structural studies of fatty acyl-(acyl carrier protein) thioesters reveal a hydrophobic binding cavity that can expand to fit longer substrates. *J. Mol. Biol.* **2007**, 365 (1), 135–145.
- (13) Cronan, J. E. Molecular-Properties of Short Chain Acyl Thioesters of Acyl Carrier Protein. *J. Biol. Chem.* **1982**, 257 (9), 5013–5017
- (14) Sztain, T.; Bartholow, T. G.; Lee, D. J.; Casalino, L.; Mitchell, A.; Young, M. A.; Wang, J. N.; McCammon, J. A.; Burkart, M. D. Decoding allosteric regulation by the acyl carrier protein. *Proc. Natl. Acad. Sci. U.S.A.* **2021**, *118* (16), No. e2025597118.
- (15) Tamara, S.; den Boer, M. A.; Heck, A. J. R. High-Resolution Native Mass Spectrometry. *Chem. Rev.* **2022**, 122 (8), 7269–7326.
- (16) Leney, A. C.; Heck, A. J. R. Native Mass Spectrometry: What is in the Name? *J. Am. Soc. Mass. Spectrom.* **2017**, 28 (1), 5–13.
- (17) Bennett, J. L.; Nguyen, G. T. H.; Donald, W. A. Protein-Small Molecule Interactions in Native Mass Spectrometry. *Chem. Rev.* **2022**, 122 (8), 7327–7385.
- (18) Bai, Y.; Liu, Z. Y.; Li, Y. Q.; Zhao, H.; Lai, C.; Zhao, S.; Chen, K. X.; Luo, C.; Yang, X. M.; Wang, F. J. Structural Mass Spectrometry Probes the Inhibitor-Induced Allosteric Activation of CDK12/CDK13-Cyclin K Dissociation. *J. Am. Chem. Soc.* **2023**, *145* (21), 11477–11481.
- (19) Luo, P.; Liu, Z. Y.; Lai, C.; Jin, Z. X.; Wang, M. D.; Zhao, H.; Liu, Y.; Zhang, W. Q.; Wang, X. G.; Xiao, C. L.; Yang, X. M.; Wang, F. J. Time-Resolved Ultraviolet Photodissociation Mass Spectrometry Probes the Mutation-Induced Alterations in Protein Stability and Unfolding Dynamics. J. Am. Chem. Soc. 2024, 146 (13), 8832–8838.
- (20) Shaw, J. B.; Li, W. Z.; Holden, D. D.; Zhang, Y.; Griep-Raming, J.; Fellers, R. T.; Early, B. P.; Thomas, P. M.; Kelleher, N. L.; Brodbelt, J. S. Complete Protein Characterization Using Top-Down Mass Spectrometry and Ultraviolet Photodissociation. *J. Am. Chem. Soc.* 2013, 135 (34), 12646–12651.
- (21) Brodbelt, J. S.; Morrison, L. J.; Santos, I. Ultraviolet Photodissociation Mass Spectrometry for Analysis of Biological Molecules. *Chem. Rev.* **2020**, *120* (7), 3328–3380.
- (22) Zhou, L.; Liu, Z.; Guo, Y.; Liu, S.; Zhao, H.; Zhao, S.; Xiao, C.; Feng, S.; Yang, X.; Wang, F. Ultraviolet Photodissociation Reveals the Molecular Mechanism of Crown Ether Microsolvation Effect on the Gas-Phase Native-like Protein Structure. *J. Am. Chem. Soc.* **2023**, *145* (2), 1285–1291.
- (23) Macias, L. A.; Santos, I. C.; Brodbelt, J. S. Ion Activation Methods for Peptides and Proteins. *Anal. Chem.* **2020**, 92 (1), 227–251
- (24) Yang, S. R.; Hou, Z. H.; Liu, Z. Y.; Jin, Z. X.; Zhao, H.; Cao, K. M.; Zhao, S.; Zhang, W. Q.; Xiao, C. L.; Yang, X. M.; Huang, G. M.; Wang, F. J. In-Cell Mass Spectrometry and Ultraviolet Photodissociation Navigates the Intracellular Protein Heterogeneity. *J. Am. Chem. Soc.* **2025**, *147* (6), 4714–4719.
- (25) Morrison, L. J.; Brodbelt, J. S. 193 nm Ultraviolet Photodissociation Mass Spectrometry of Tetrameric Protein Complexes Provides Insight into Quaternary and Secondary Protein Topology. J. Am. Chem. Soc. 2016, 138 (34), 10849–10859.
- (26) Liu, Z.; Yang, S.; Zhou, L.; He, M.; Bai, Y.; Zhao, S.; Wang, F. Structural characterization of protein-material interfacial interactions using lysine reactivity profiling-mass spectrometry. *Nat. Protoc.* **2023**, 18 (8), 2600–2623.
- (27) Kaltashov, I. A.; Eyles, S. J. Studies of biomolecular conformations and conformational dynamics by mass spectrometry. *Mass Spectrom. Rev.* **2002**, *21* (1), 37–71.

- (28) Cammarata, M. B.; Brodbelt, J. S. Structural characterization of holo- and apo-myoglobin in the gas phase by ultraviolet photo-dissociation mass spectrometry. *Chem. Sci.* **2015**, *6* (2), 1324–1333.
- (29) Cammarata, M. B.; Schardon, C. L.; Mehaffey, M. R.; Rosenberg, J.; Singleton, J.; Fast, W.; Brodbelt, J. S. Impact of G12 Mutations on the Structure of K-Ras Probed by Ultraviolet Photodissociation Mass Spectrometry. *J. Am. Chem. Soc.* **2016**, *138* (40), 13187–13196.
- (30) Kim, Y.; Kovrigin, E. L.; Eletr, Z. NMR studies of acyl carrier protein: Dynamic and structural differences of the apo- and holoforms. *Biochem. Biophys. Res. Commun.* **2006**, 341 (3), 776–783.
- (31) Li, Q.; Khosla, C.; Puglisi, J. D.; Liu, C. W. Solution structure and backbone dynamics of the holo form of the frenolicin acyl carrier protein. *Biochem.* **2003**, *42* (16), 4648–4657.
- (32) Arya, R.; Sharma, B.; Dhembla, C.; Pal, R. K.; Patel, A. K.; Sundd, M.; Ghosh, B.; Makde, R. D.; Kundu, S. A conformational switch from a closed apo- to an open holo-form equips the acyl carrier protein for acyl chain accommodation. *Biochim. Biophys. Acta Proteins Proteom.* **2019**, *1867* (3), 163–174.
- (33) Evans, S. E.; Williams, C.; Arthur, C. J.; Burston, S. G.; Simpson, T. J.; Crosby, J.; Crump, M. P. An ACP Structural Switch: Conformational Differences between the Apo and Holo Forms of the Actinorhodin Polyketide Synthase Acyl Carrier Protein. *ChemBio-Chem.* 2008, 9 (15), 2424–2432.
- (34) Zhang, X. Y.; Zhang, H.; Guan, S. S.; Luo, Z. J.; Jingwen, E.; Yang, Z. J.; Du, J.; Wang, S. Studies on the Selectivity Mechanism of Wild-Type Thioesterase 'TesA and Its Mutants for Medium- and Long-Chain Acyl Substrates. *Catalysts* **2022**, *12* (9), 1026.
- (35) Noga, M. J.; Büke, F.; van den Broek, N. J. F.; Imholz, N. C. E.; Scherer, N.; Yang, F.; Bokinsky, G.; Stephen Trent, M. Posttranslational Control of PlsB Is Sufficient To Coordinate Membrane Synthesis with Growth in Escherichia coli. *mBio* **2020**, *11* (4), No. e02703-19.
- (36) Ploskon, E.; Arthur, C. J.; Kanari, A. L. P.; Wattana-amorn, P.; Williams, C.; Crosby, J.; Simpson, T. J.; Willis, C. L.; Crump, M. P. Recognition of Intermediate Functionality by Acyl Carrier Protein over a Complete Cycle of Fatty Acid Biosynthesis. *Chem. Biol.* **2010**, 17 (7), 776–785.
- (37) Wu, B. N.; Zhang, Y. M.; Rock, C. O.; Zheng, J. J. Structural modification of acyl carrier protein by butyryl group. *Protein Sci.* **2009**, *18* (1), 240–246.
- (38) Rock, C. O. Environment of the Aromatic Chromophores of Acyl Carrier Protein. *Arch. Biochem. Biophys.* **1983**, 225 (1), 122–129.
- (39) Parris, K. D.; Lin, L.; Tam, A.; Mathew, R.; Hixon, J.; Stahl, M.; Fritz, C. C.; Seehra, J.; Somers, W. S. Crystal structures of substrate binding to holo-(acyl carrier protein) synthase reveal a novel trimeric arrangement of molecules resulting in three active sites. *Structure* **2000**, *8* (8), 883–895.
- (40) Chan, D. I.; Stockner, T.; Tieleman, D. P.; Vogel, H. J. Molecular Dynamics Simulations of the Apo-, Holo-, and Acyl-forms of Acyl Carrier Protein. *J. Biol. Chem.* **2008**, 283 (48), 33620–33629.
- (41) Milligan, J. C.; Lee, D. J.; Jackson, D. R.; Schaub, A. J.; Beld, J.; Barajas, J. F.; Hale, J. J.; Luo, R.; Burkart, M. D.; Tsai, S. C. Molecular basis for interactions between an acyl carrier protein and a ketosynthase. *Nat. Chem. Biol.* **2019**, *15* (7), 669–671.
- (42) Buyachuihan, L.; Stegemann, F.; Grininger, M. How Acyl Carrier Proteins (ACPs) Direct Fatty Acid and Polyketide Biosynthesis. *Angew. Chem., Int. Ed.* **2024**, 63 (4), No. e202312476.
- (43) Zornetzer, G. A.; Fox, B. G.; Markley, J. L. Solution structures of spinach acyl carrier protein with decanoate and stearate. *Biochem.* **2006**, 45 (16), 5217–5227.